



Variations of central pressure of intense tropical cyclones over the Bay of Bengal with latent heat flux and other parameters

PRAVAT RABI NASKAR^{1,*}  and DUSHMANTA RANJAN PATTANAİK²

¹*Meteorological office Port Blair, India Meteorological Department, Ministry of Earth Sciences, Port Blair 744 106, India.*

²*Office of the Director-General of Meteorology, India Meteorological Department, Ministry of Earth Sciences, New Delhi 110 003, India.*

*Corresponding author. e-mail: pravat091@gmail.com

MS received 10 December 2021; revised 7 September 2022; accepted 25 November 2022

This study aims to find out the variations of central pressure (intensity) of intense tropical cyclones (TCs) with sea surface temperature (SST), mid-tropospheric relative humidity (MRH), mid-tropospheric instability (MI), vertical wind shear (VWS), 200 hPa divergence, and surface latent heat flux (SLHF) during the lifetime of intense TCs, and determine the most crucial parameter which shows the highest correlation with central pressure (intensity). Out of all these parameters, SLHF is highly correlated ($R^2 = 0.74$) with the central pressure of intense TCs. Increase and decrease of SLHF correspond to decrease and increase of TCs central pressure (increase and decrease in TCs intensity). The highest SLHF corresponds to the lowest central pressure (highest intensity).

Keywords. Intense tropical cyclones; latent heat flux; Bay of Bengal; genesis; intensification; ERA5.

1. Introduction

Tropical cyclones (TCs) are one of the most destructive weather phenomena in the world. They cause human fatalities, structural damages, and economic losses worldwide (Pielke and Pielke 1997; Simpson *et al.* 2002; Manganello *et al.* 2012). They are large-scale rotary systems that originate over warm ocean waters in tropical or sub-tropical regions (Montgomery and Farrell 1993). They are associated with organized convections and have surface wind speeds of 34 knots or more for at least one 6-h period (Bhardwaj and Singh 2020). On average North Indian Ocean (NIO), including the Bay of Bengal (BoB) and Arabian Sea (AS),

accounts for 7% of the global TCs (Neumann 1993). India is affected mainly by the TCs, which develop in the NIO, including the BoB and the AS. About 80% of these cyclones form in the BoB (Singh 2007), which tend to be the deadliest of any TCs around the globe. They develop in the pre-monsoon and post-monsoon seasons and generally move west-northwestwards to northwestwards (Chinchole and Mohapatra 2017). The average life period and frequencies of these TCs over BoB are 4–5 days and 4, respectively (Mohapatra *et al.* 2014; Kumar *et al.* 2017). India Meteorological Department (IMD) classifies TCs into five categories based on their wind speeds, starting from the cyclonic storm (CS) to the super cyclonic storm

(SuCS). Very severe cyclonic storms (VSCS), extremely severe cyclonic storms (ESCS), and SuCS are the most destructive and intense TCs. Therefore, their genesis, intensification, and track are of particular significance.

Various atmospheric conditions such as strong vertical wind shear, mid-tropospheric instability and mid-tropospheric humidity influence TCs genesis and intensification. Many scientists (Gray 1968, 1979; DeMaria 1996; Emanuel *et al.* 2004; Kotal *et al.* 2009; Ganesh *et al.* 2020; Sanap *et al.* 2020; Naskar and Naskar 2021) have previously worked to find out the role of these parameters in TCs genesis and intensification. Many previous studies (Reihl 1950; Ooyama 1969; Emanuel 1986; Vinod *et al.* 2014; Lengaigne *et al.* 2019; Naskar and Naskar 2021; Singh and Roxy 2022) have also brought out the crucial role played by air–sea interaction processes in tropical cyclone genesis and intensification. As TCs primarily draw their energy from evaporation at the ocean surface, the latent heat fluxes at the air–sea interface also play an essential role in TCs intensification (Montgomery *et al.* 2009; Gao and Chiu 2010; Andersen *et al.* 2013; Chen *et al.* 2014; Zhou *et al.* 2015; Srinivas *et al.* 2016; Naskar and Naskar 2021; Singh and Roxy 2022). Moreover, the genesis and intensification characteristics of TCs differ from ocean basin to ocean basin (Flotz *et al.* 2018). Despite the above studies, the prediction of TCs genesis and intensification is still a challenge. This implies that the processes behind TCs genesis and intensification are yet to be understood. Many recent studies on TCs over BoB show that scientists have focused on a few individual dynamical and thermo-dynamical parameters to describe the genesis and intensification (Mohanty *et al.* 2019; Reshmi Mohan *et al.* 2022; Vishwakarma *et al.* 2022). Mohanty *et al.* (2019) observed a crucial role of SST in modulating the life cycle of TCs over BoB. Vishwakarma *et al.* (2022) observed that Amphan experienced rapid cooling during rapid intensification. Reshmi Mohan *et al.* (2022) observed anomalously high MRH (10–40%), upper atmospheric divergence ($0\text{--}10 \times 10^{-5} \text{ s}^{-1}$), low-level cyclonic vorticity ($10\text{--}50 \times 10^{-5} \text{ s}^{-1}$), and moderate shear before intensification of Amphan and Fani. They also observed higher positive SST anomaly, strong diabatic heating and increased surface fluxes during the rapid intensification of Amphan and Fani which indicates positive warm SST feedback. Sanap *et al.* (2020) observed that the regions of anomalously high SST, subsurface temperatures,

tropical cyclone heat potential (TCHP) and ocean mean temperature (OMT) with a depth of 26°C isotherms up to 100 m favoured rapid intensification of TC Ockhi. Singh *et al.* (2020) showed that Madden Julian oscillation (MJO) and warm oceanic conditions helped in the genesis of Ockhi, and favourable thermodynamic conditions due to warm SST helped its intensification. Harikumar *et al.* (2022) observed that vorticity and RH were more favourable than VWS and potential intensity before the genesis of Ockhi and they suggested that forecasters should consider the background dynamic and thermodynamic conditions extensively in addition to model guidance for better prediction of genesis, intensity and track of TCs. Ahmed *et al.* (2021) observed the characteristic features of Super Cyclone Amphan through satellite images and concluded that precise changes in geometric and thermal characteristics of the ‘eye’ of Amphan are related to its intensity and these eye features can be used for very short range intensity prediction of a TC. Mohapatra and Sharma (2021) compared some vital parameters including location, movement, intensity, size, etc. for ‘Phailin’ and ‘Hudhud’ and found that higher intensity, higher rate of intensification, longer duration, lower rate of decay after landfall and larger size were responsible for higher damage potential. Most of these studies are limited to case study specific or a small group of TCs. The present study considers most of the important dynamic and thermodynamic parameters and latent heat flux for a large group of intense TCs. This study aims to find out the correlation of these parameters with TCs intensity (central pressure/maximum sustained wind speed) as well as the correlation among themselves during the life period of TCs. This will help find the most important parameter for genesis and intensification.

2. Data and methodology

The study region under consideration is BoB ($0^\circ\text{--}31^\circ\text{N}$, $79^\circ\text{--}111^\circ\text{E}$). Three hourly $0.25^\circ \times 0.25^\circ$ resolution European Center for Medium-Range Forecasts (ECMWF) ERA5 reanalysis data (Hersbach and Dee 2016) for the parameters such as wind speed and direction, temperature, relative humidity at different pressure levels, mean sea level pressure (MSLP), 200 hPa divergence, SST and SLHF for the period 1990–2019 have been obtained and used in this study. Past studies have

shown that the ERA5 dataset well represents the evolution and many observed features of tropical cyclones (Malakar *et al.* 2020; Sanap *et al.* 2020; Bian *et al.* 2021). But ERA5 dataset is model-derived and not pure observation-based; hence for comparison purposes, we have taken three hourly $0.5^\circ \times 0.625^\circ$ total latent energy flux (TLEF) and wind speed data of Modern-Era Retrospective Analysis for Research and Application, version 2 (MERRA2) (Gelaro *et al.* 2017) which is derived based on satellite remote sensing. Best track data of intense TCs for the period 1990–2019 have been collected from RSMC New Delhi for the track, wind speed, and MSLP. Here VSCS (maximum wind speed 64–89 kts), ESCS (90–119 kts), and SuCS (120 kts and above) have been termed intense TCs. Here we have considered several dynamic and thermodynamic parameters of TCs. The dynamic parameters are 200 hPa divergence and VWS. The thermodynamic parameters are SST, MI, MRH, TLEF and SLHF. The VWS has been calculated by taking the difference of 200 and 850 hPa winds. MRH is the mean relative humidity between 700 and 500 hPa, mid-tropospheric instability (MI) has been calculated by using $MI = (T_{850} - T_{500})^\circ C$, where T_{850} and T_{500} are the temperatures at 850 and 500 hPa, respectively. The parameters such as max SLHF, max TLEF, min VWS, min MSLP, max 200 hPa divergence, mean SST, mean MI, and mean MRH have been calculated within a $6^\circ \times 6^\circ$ box centering the eye of the cyclone. The composite mean of SLHF has been calculated by taking the mean of SLHFs of all TCs during their lifetime. SLHF is positive downward and negative upward. SLHF is generally denoted with a negative sign unless there is a downward energy transfer. Pearson’s correlation method has been used to derive the correlation among the parameters.

3. Results and discussions

In this study, 31 intense TCs which originated in the BoB from 1990 to 2019 have been analyzed. Figure 1 shows the genesis and landfall locations of intense TCs during this period. The red stars, dots, and triangles correspond to the genesis locations of SuCS, ESCS, and VSCS, respectively, and blue stars, dots, and triangles correspond to the landfall locations of SuCS, ESCS, and VSCS, respectively. Figure 2 shows the latitudinal and longitudinal distribution of these TCs. It is clear from

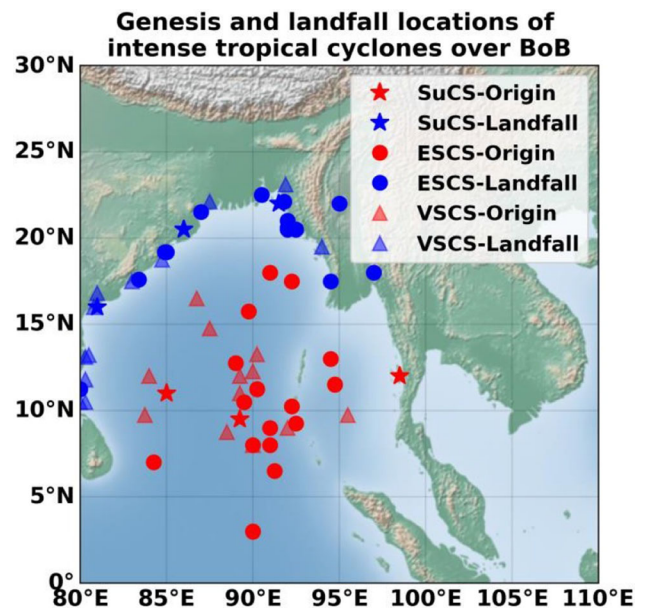


Figure 1. Genesis and landfall locations of intense TCs over BoB.

figure 2(a) that almost 75% of these TCs originate between 8° and $14^\circ N$, and from figure 2(b), nearly 65% of these TCs originate between 88° and $94^\circ E$. It is also seen that almost 60% of these TCs develop within the latitude/longitude box 8° – $14^\circ N$ and 88° – $94^\circ E$. Figure 3(b) shows the seasonal variations of these TCs. It is seen that almost 70% of these TCs form in the post-monsoon season and 30% form in the pre-monsoon season. Figure 3(c) exhibits the monthly variations of these TCs. It is observed that October month experiences the most of these TCs and it is nearly 35%. No intense TC has been formed in January, February, March, June, July, August, and September. Figure 3(a) shows the frequencies of intense TCs to their maximum SLHF values. It is observed that the frequency of TCs with SLHF values 1100 – 1400 KJ/m^2 is maximum and above 2000 KJ/m^2 is minimum.

During the intensification of a tropical cyclone, the central pressure falls. Central pressure is one of the most reliable measures of TCs intensity (Chavas *et al.* 2017). Maximum sustained wind speed is also another important parameter for TCs intensity characterization. In fact, India Meteorological Department (IMD) categorizes TCs over NIO based on maximum sustained 10 m wind speed. Bhardwaj and Singh (2020) showed that the decrease in the central pressure of TCs and the increase in 10 m surface wind speed is proportional with a correlation coefficient of 0.97. In this study, central pressure, as well as maximum wind speed

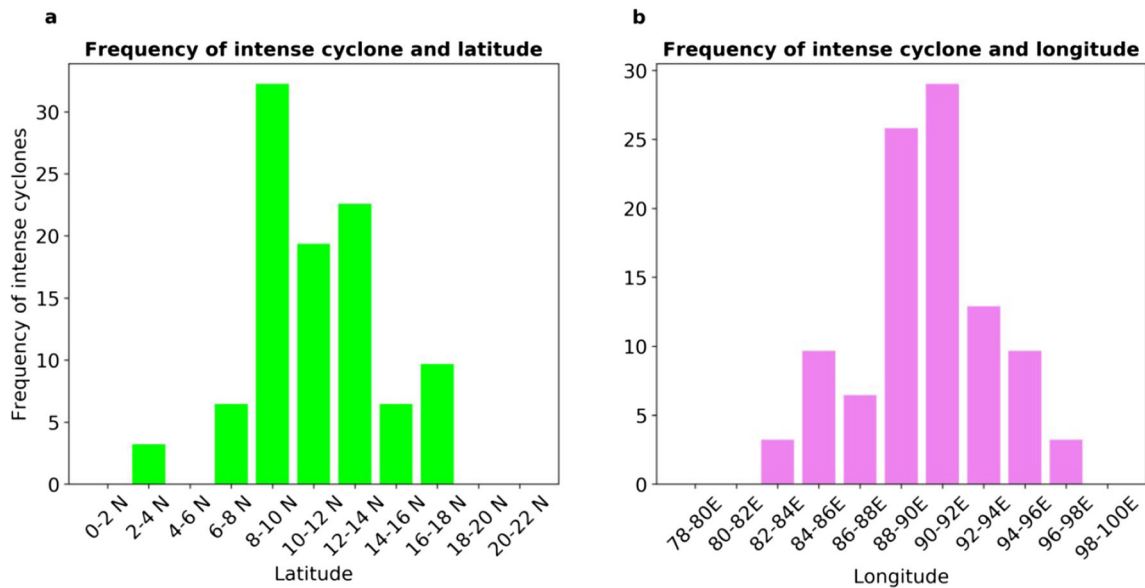


Figure 2. (a) Latitudinal and (b) longitudinal variations of intense TCs over BoB.

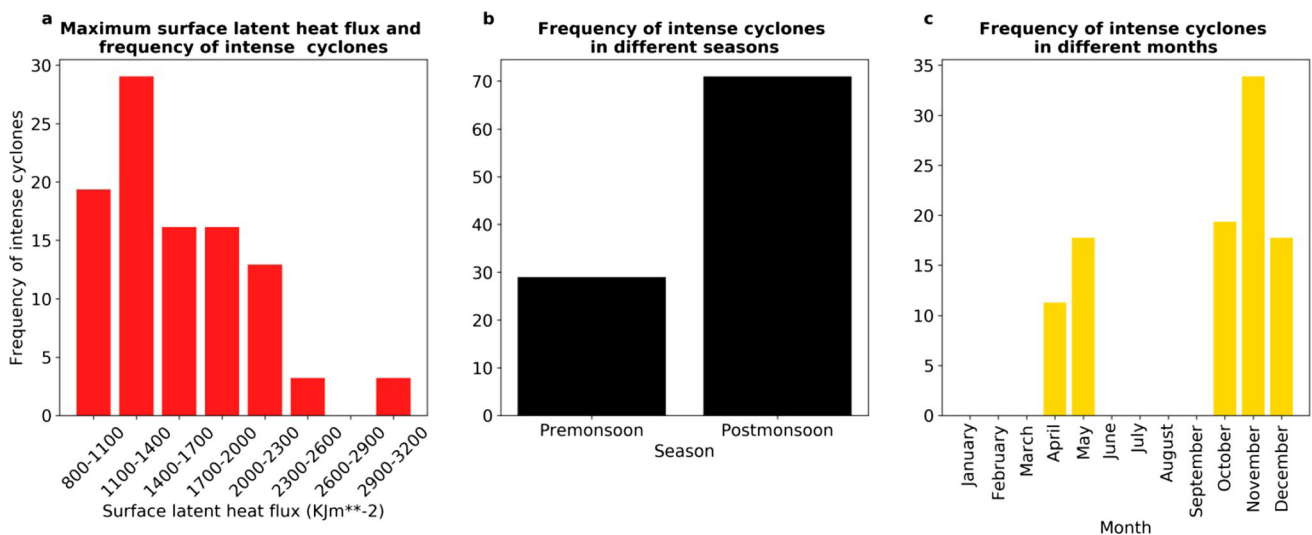


Figure 3. (a) Variations of frequency of intense TCs and maximum SLHF, (b) seasonal variations of intense TCs and (c) monthly variations of intense TCs.

during the lifetime of TCs, have been plotted against the parameters such as SST, SLHF, 200 hPa divergence, MRH, and MI to observe if there is any relation between central pressure/maximum wind speed with these parameters during the entire life period of TCs.

Warm oceans ($SST > 26.5^{\circ}\text{C}$) are favourable for the genesis of TCs (Palmen 1948; Gray 1998). They act as the source of energy for TCs. Using a high-resolution regional model (Lavender *et al.* 2018) showed that an increase (decrease) in SST was associated with an increase (decrease) in TC intensity. Ren *et al.* (2014) analyzed the influence

of SST on TCs over four basins (Western North Pacific, North Atlantic Ocean, South Indian Ocean/Northwest Western Australian Ocean, and Southwest Pacific) and found that the intensities of TCs increased with increasing SST and warmer SST indicated more rapid intensification. Sun *et al.* (2017) showed that under the SST warming, TCs not only became stronger but also more prominent. Naskar and Naskar (2021) observed that under favourable conditions, abnormally high SST had rapidly intensified SuCS Amphan. Keeping in mind the influence of SST on TCs intensity as stated above, central pressures/max wind speed of all TCs

have been plotted against SST values during TCs' lifetime for the period 1990–2019 in figures 4(a)/ 5(a), respectively. It is seen that SST does not show any significant relation with central pressure (max wind). Though it is observed that higher SST corresponds to lower central pressure (higher max wind speed) for some intense TCs but not for all. The R^2 value is -0.37 (0.31). The reason behind this may be TC-induced cooling. When a TC moves over the warm ocean, it reduces the SST along its track, mainly through vertical mixing and upwelling (Vincent *et al.* 2012a, b). Generally, SST remains high during the early stage of a TC and decreases with time during its lifetime. This has been observed by previous studies (Sanap *et al.* 2020; Naskar and Naskar 2021). If we take an area

average value of SST at this genesis stage, that will be comparatively higher than the mature or dissipation stage. Whereas the pressure (max wind speed) will be comparatively higher (lower) during the early or dissipation stage than in the mature stage. This may result in higher central pressure (lower max wind speed) corresponding to higher SST (in the early stage), lower central pressure (higher max wind speed) corresponding to lower SST (in the mature stage) and higher central pressure (lower max wind speed) corresponding to lower SST (in dissipation stage). Hence in this study, it is not clear whether SST is responsible for the intensity change of TCs during their life period.

Upper-level divergence is an essential parameter for TCs intensification. It acts as the outflow in the

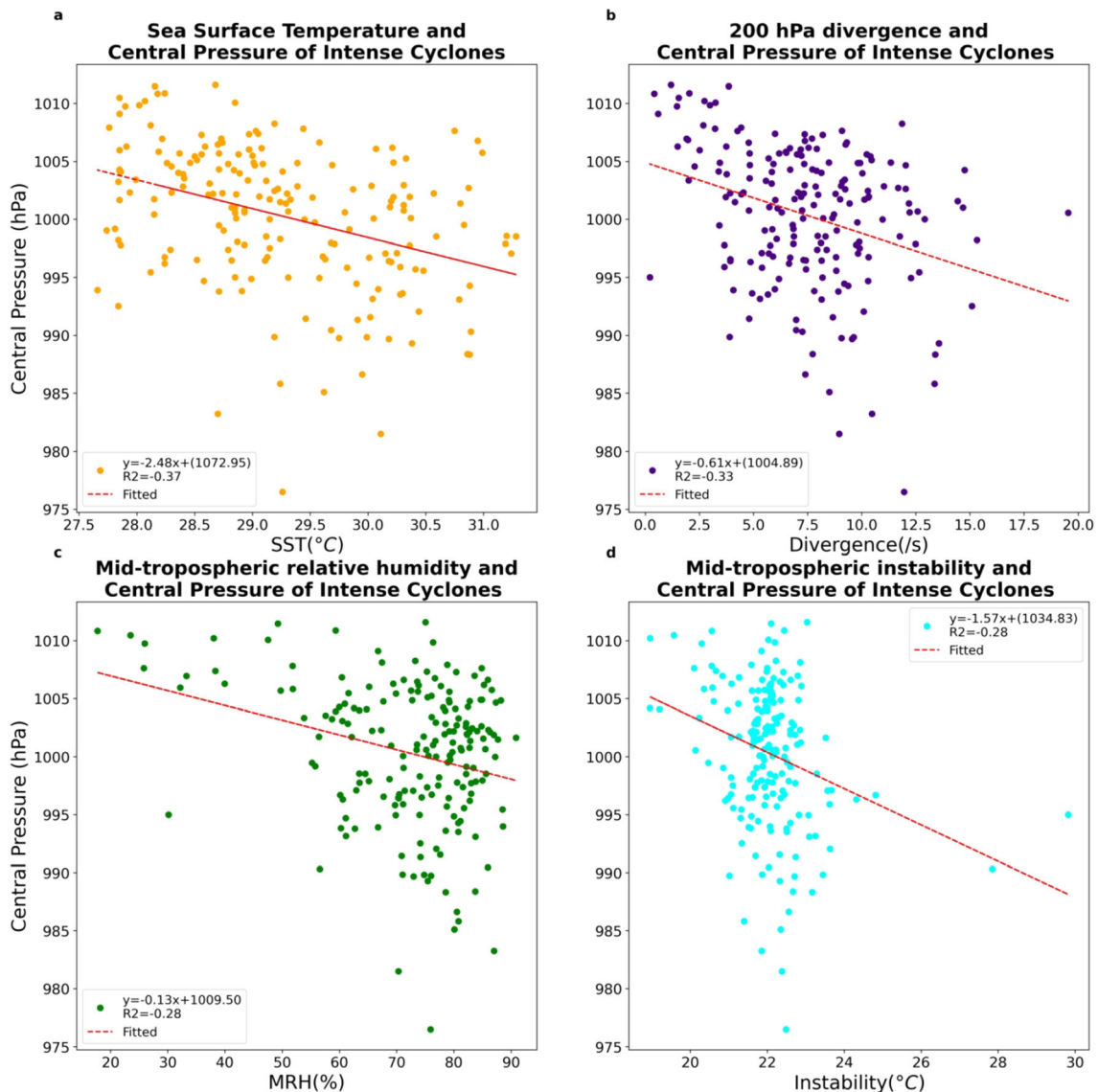


Figure 4. Variations of central pressure of intense TCs with (a) SST, (b) 200 hPa divergence, (c) mid-tropospheric relative humidity and (d) mid-tropospheric instability.

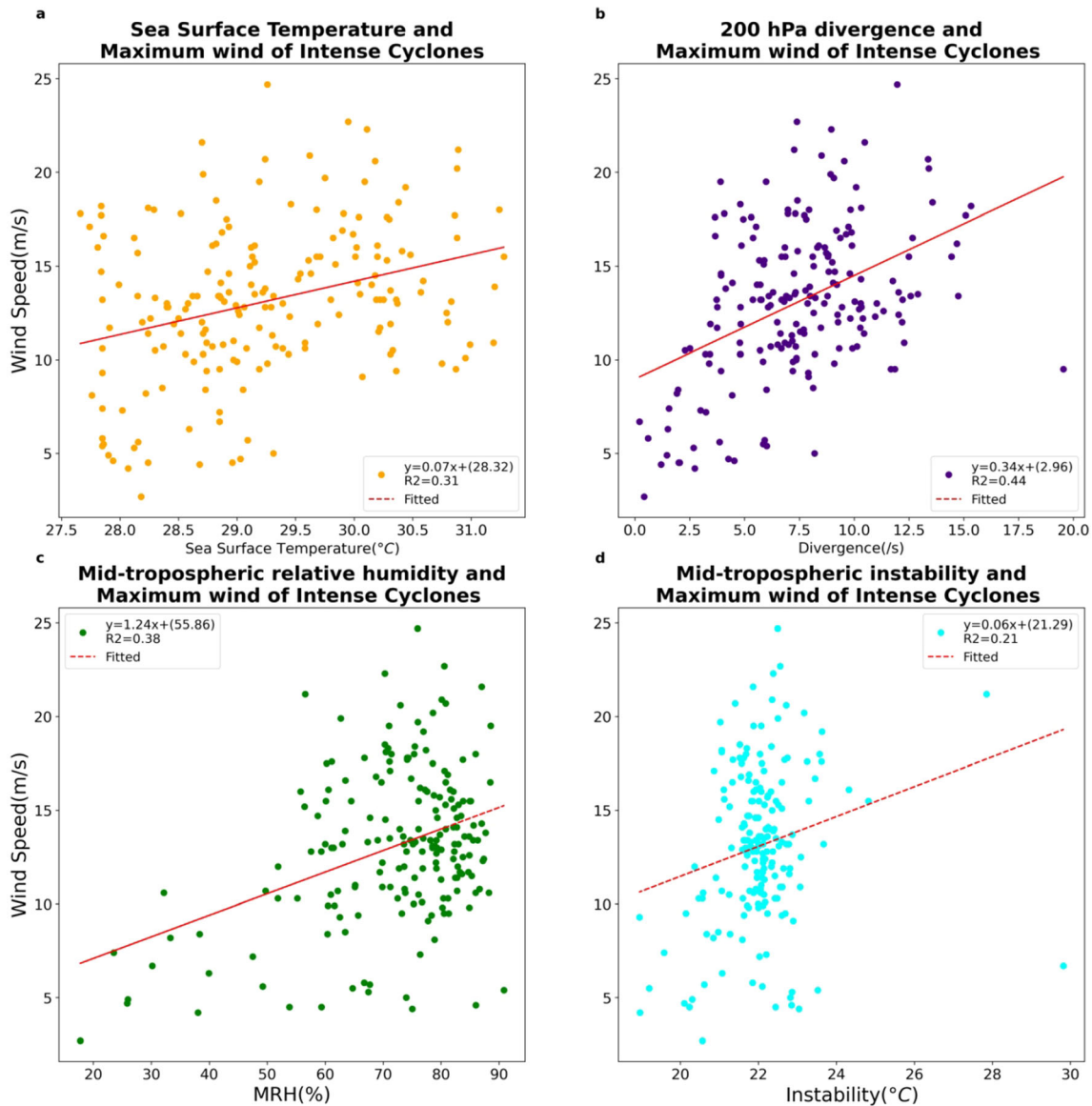


Figure 5. Variations of wind speed of intense TCs with (a) SST, (b) 200 hPa divergence, (c) mid-tropospheric relative humidity and (d) mid-tropospheric instability.

upper level. Rappin *et al.* (2011) opined that an outflow layer in the upper level could modify TC's core structure so that TC outflow could access weak inertial stability in the environment, which minimized an energy sink of the tropical cyclone secondary circulation and led to rapid intensification. Naskar and Naskar (2021) showed that 200 hPa divergence reached its peak during the maximum intensity of SuCS Amphan. In figures 4(b)/5(b), central pressures/max wind speed of all TCs have been plotted against 200 hPa divergence values during TCs' lifetime for the period 1990–2019. It is seen that there is a decreasing (increasing) trend of 200 hPa divergence with central pressure (max wind speed) of TCs. But this trend is not uniform as many points show the high

divergence corresponding to high central pressure (low max wind speed) and low central pressure (high max wind speed) corresponding to low divergence; the R^2 value is -0.33 (0.44). This may be due to the divergence variations at different stages of TCs. Generally, during genesis moderate divergence, during intensification maximum divergence, and during decay weak divergence/convergence is observed (Naskar and Naskar 2021). This means the magnitude of divergence at depression during genesis will be comparatively higher than the magnitude of divergence at depression during decay. Moreover, divergence is also not uniform to central pressure/max wind during intensification in all TCs. The reason behind this is not apparent. We have tried to find

out the relations between TCs intensity and divergence at different stages (figures not shown) but not found any significant correlation in the respective stages.

MRH and MI (Instability) are also essential factors for the genesis and intensification of TCs (Gray 1979; Kotal *et al.* 2009). High MRH ensures the moistening of the middle troposphere and helps TC's intensification. Kotal *et al.* (2009) showed that MRH first increased slightly and then became stable during their lifetime for developing systems. The genesis of TCs is characterized by intense convective activity, which is associated with MI. It is the temperature difference between 850 and 500 hPa. It increases during the initial stages of TCs and then decreases (Kotal *et al.* 2009). Figures 4(c)/5(c) and 4(d)/5(d) show the variations of central pressure/max wind with MRH and MI. Though there are decreasing (increasing) trends of central pressure (max wind) with MRH and MI, they are not significant. The R^2 values corresponding to TCs central pressure and max wind to MRH are -0.28 and 0.38 , respectively. The R^2 values corresponding to TCs central pressure and max wind to MI are -0.28 and 0.21 , respectively. This may be because the values of MRH and MI do not change much during the lifetime of TCs. Most of the values of MRH and MI are between 70–95% and 21–23°C, respectively, during the lifetime of TCs. This suggests that though a certain amount of MRH and MI is required for the genesis and intensification, they are not explicitly related to the intensity variations of TCs during their lifetime.

VWS is also an essential factor for the genesis (Gray 1968) and intensification of TCs. It is the primary environmental control during the formation and early intensification stage over regions of significant ocean heat content (Park *et al.* 2012). Low VWS acts in initiating a conducive environment for cyclone movement and sustainment. Generally, VWS remains low and does not change much throughout the lifetime of a TC except in the dissipation stage (landfall). Its values remain within 5–10 m/s for most of the TCs. The relationship of VWS with central pressure/max wind has not been shown here. But from the correlation matrix (figure 9) it is seen that the relation between VWS and TCs intensity (central pressure/max wind) is not significant. The R^2 values corresponding to VWS and TCs central pressure and max wind based on the ERA5 data are -0.16 and 0.14 , respectively.

SLHF transfers latent heat (resulting from water phase changes, such as evaporation and condensation) between Earth's surface and the atmosphere through turbulent air motion (Naskar and Naskar 2021). It plays a vital role in the ocean surface energy balance. It is the primary source of energy fueling TC development (Ooyama 1969) and intensification. It can provide convective instability and help develop convective activity (Cheng and Wu 2020). Like other parameters, the variations of central pressure and max wind with SLHF have also been examined. There are two seasons for TCs genesis over BoB; namely pre-monsoon and post-monsoon, the variations of central pressure with SLHF in pre-monsoon and post-monsoon seasons have been plotted separately to observe if there is any difference in the relationship during these seasons. Figure 6(a) shows a significant relationship between central pressure and SLHF for the entire period. It is seen that when there is a strong upward release of latent heat energy in the form of surface latent heat flux, the central pressure is minimum and vice versa. The variations of central pressure with the SLHF in different seasons, as depicted in figure 6(b and c) are also significant ($R^2 = 0.64$ and 0.72) and show the same trend as figure 6(a). However, from figure 6(b and c), it is observed that SLHF is higher in the pre-monsoon season than in the post-monsoon season. This may be due to higher SST in the pre-monsoon season. The variation of SLHF with the max wind in figure 7(a) depicts a very high correlation ($R^2 = -0.81$) in fact, this is a little higher than that with central pressure ($R^2 = 0.74$). We have also compared this result with satellite-derived MERRA2-TLEF and MERRA2-max wind. MERRA2-max wind *vs.* MERRA2-TLEF in figure 7(b) also shows a very high correlation (0.62). This indicates a significant relationship between SLHF/TLEF with TCs intensity. It shows that the higher the SLHF value, the lower the central pressure (higher is the max wind). The reason may be due to the 'evaporation-wind' feedback mechanism known as wind-induced surface heat exchange (WISHE) (Emanuel 1994; Emanuel *et al.* 1994; Montgomery *et al.* 2009; Zhang and Emanuel 2016; Cheng and Wu 2020). We have also shown the correlation between ERA-wind and MERRA-wind in figure 7(c) to compare the ERA and MERRA winds during the lifetime of intense TCs. It is observed that the correlation between ERA-wind and MERRA-wind is very high ($R^2 = 0.80$). This indicates that model-derived

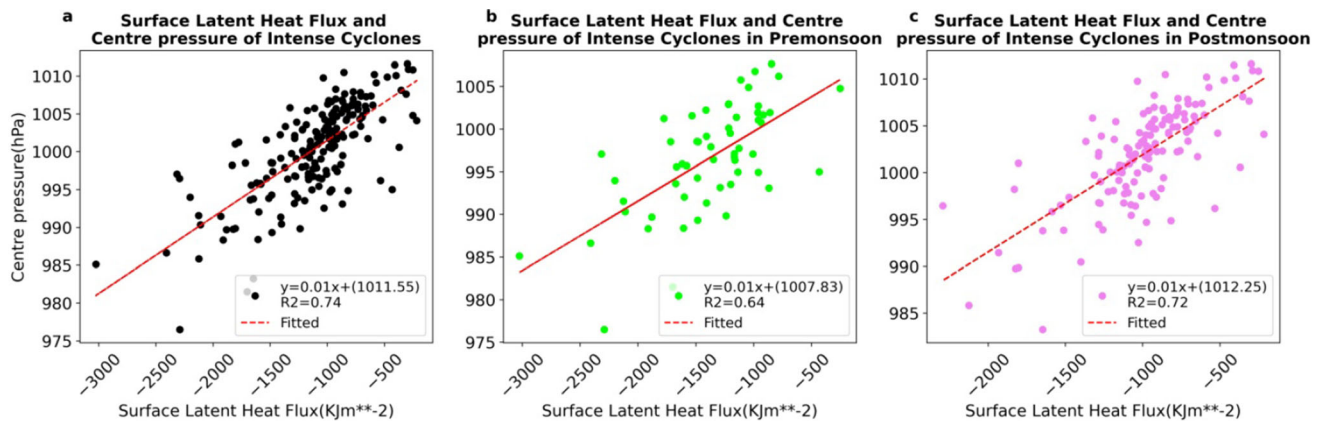


Figure 6. Variations of central pressure of intense TCs with SLHF during (a) all the season, (b) pre-monsoon, and (c) post-monsoon.

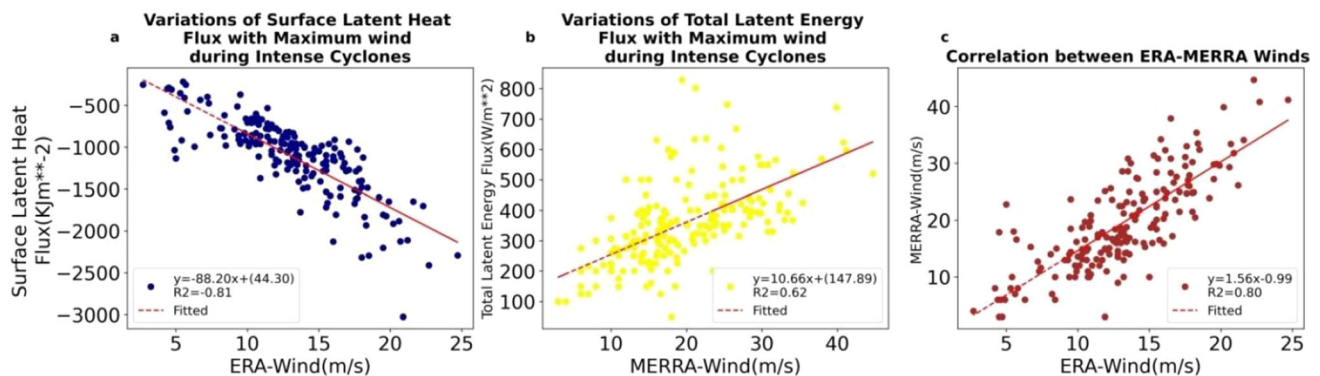


Figure 7. (a) Variations of SLHF and max ERA-wind, (b) variations of TLEF and max MERRA2-wind, and (c) correlation between max MERRA2-wind and max ERA-wind.

ERA-wind is in good agreement with satellite-derived MERRA-wind.

Scientists have observed that, generally, SLHF is closely associated with SST. Li *et al.* (2011) observed that an increase in SST directly contributes to the change in SLHF. Yu and Weller (2007) indicated that an increase in SLHF is mainly associated with an increase in SST. In this study, variation of SLHF with SST during the lifetime of TCs has been plotted in figure 8(a). It is seen that higher SLHF is associated with higher SST, but this relationship is not very accurate as many points depict lower SLHF as corresponding to higher SST. The R^2 value of the fitted line is also -0.43 . As discussed earlier, the SST value changes from high to low during a TC's lifetime. This means the SST value in the mature stage is comparatively lower than in the genesis stage. But the value of SLHF increases with an increase in TC intensity. This may be the reason behind this low correlation. It is clear that SST is weakly correlated with SLHF whereas SLHF is strongly correlated with wind speed. Hence it can be argued that

during the passage of a highly intensified cyclone over a warm-ocean and the resulting cooling of the sea surface, it is the strong aerodynamic effect under very strong winds which accelerates the evaporation process and maintains the same rate of latent flux transfer to the atmosphere.

Upper-level divergence and MI are also thought to be related to SLHF. SLHF against 200 hPa divergence and MI have been plotted in figure 8(b and c), respectively. It is seen that SLHF is higher when upper-level divergence is strong and vice versa though this relation is not significant ($R^2 = -0.30$ and 0.21). As seen earlier, the values of VWS and MI do not vary much with TC intensity. MI values are between 20 – 24°C for all values of SLHF. But the value of SLHF changes with TC intensity. The higher the SLHF value, the higher the intensity. This may be the reason behind this low correlation.

The correlation matrix in figure 9 summarizes all the relationships among the parameters (IMD-pressure, IMD-wind, ERA-wind, MERRA-wind, MERRA-TLEF, ERA-SLHF, ERA-pressure,

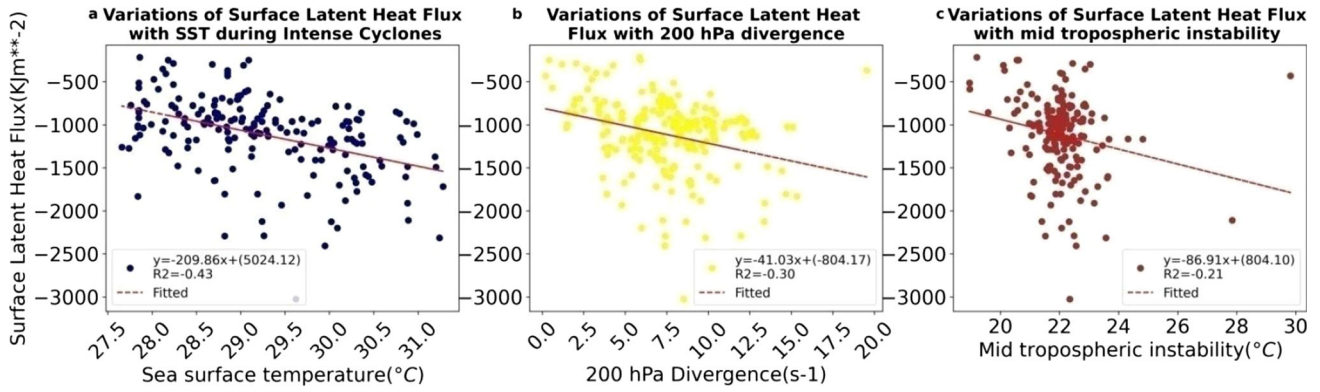


Figure 8. Variations of SLHF with (a) SST, (b) 200 hPa divergence and (c) MI.

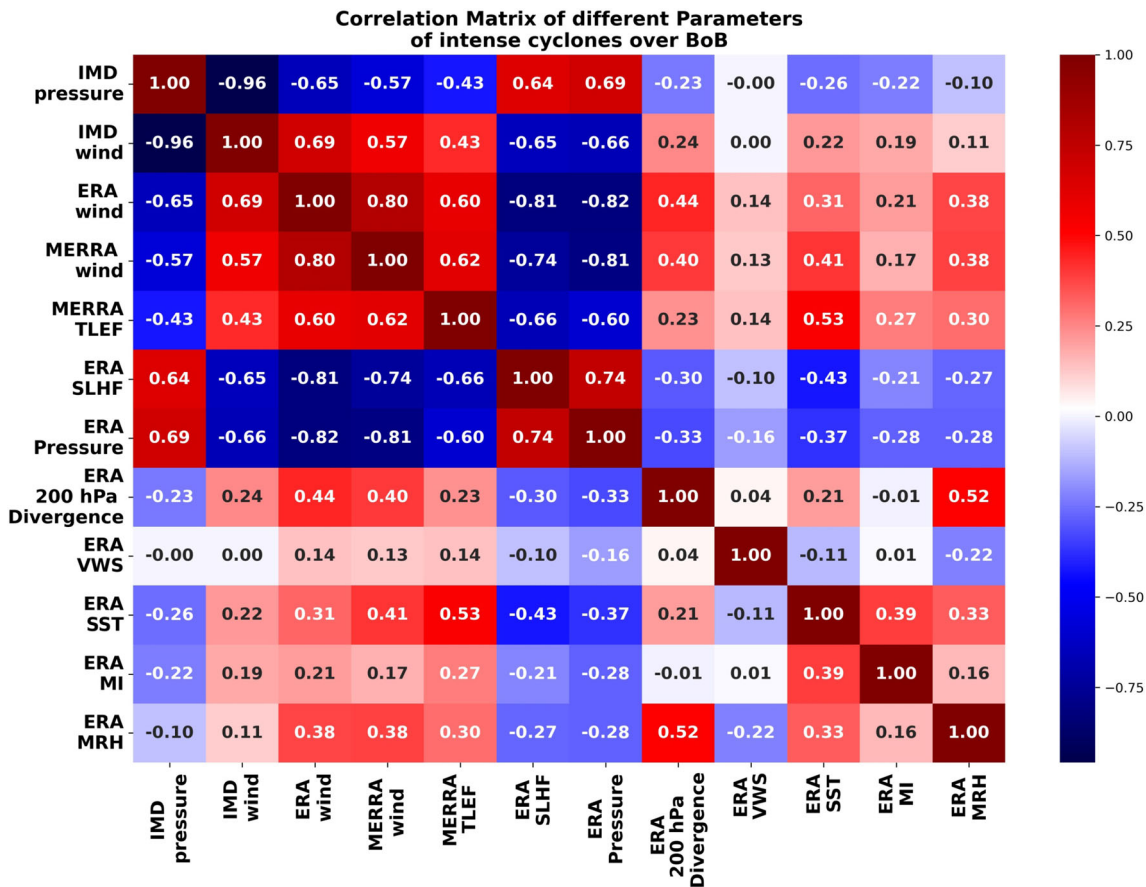


Figure 9. Correlation matrix of different parameters of intense TCs over BoB.

ERA-200 hPa divergence, ERA-VWS, ERA-SST, ERA-MI and ERA-MRH). From this matrix, we can readily find how they correlate. It is observed that ERA-SLHF has very high correlations with ERA-pressure ($R^2 = 0.74$), IMD-pressure ($R^2 = 0.64$), ERA-wind ($R^2 = -0.81$), MERRA-wind ($R^2 = -0.74$), IMD-wind ($R^2 = -0.65$) and MERRA-TLEF ($R^2 = -0.66$). It is also observed that IMD-wind is highly correlated with IMD-pressure ($R^2 =$

-0.96), ERA-wind ($R^2 = 0.69$), MERRA-wind ($R^2 = 0.57$) and ERA-pressure ($R^2 = -0.66$). It is also observed that ERA-wind is highly correlated with IMD-pressure ($R^2 = -0.65$), IMD-wind ($R^2 = 0.69$), MERRA-wind ($R^2 = 0.80$), MERRA-TLEF ($R^2 = 0.60$) and ERA-pressure ($R^2 = -0.82$). There is also a good correlation between ERA-upper-level divergence and ERA-MRH ($R^2 = 0.52$), which signifies that strong divergence in the upper level

enhances moistening in the middle troposphere. The correlations among other parameters are very small or insignificant. It is clear that during the life period of a TC, intensity is highly correlated with SLHF.

Figure 10 shows the variations of SLHF and central pressure for nine different TCs in the categories of SuCS, ESCS, and VSCS, respectively. It is seen that when central pressure is minimum (976.3 mb) the SLHF is maximum, and when

central pressure is maximum (1000.6 mb) the SLHF is minimum.

Figure 11 shows the composite mean of SLHFs during the lifetime of all TCs during the study period. In this figure, we have also overlaid the genesis locations of intense TCs on the composite mean of SLHFs. It is found that SLHF is the maximum in the regions 8–14°N and 88–94°E, which is also the location where the maximum number of the genesis of intense TCs occurs.

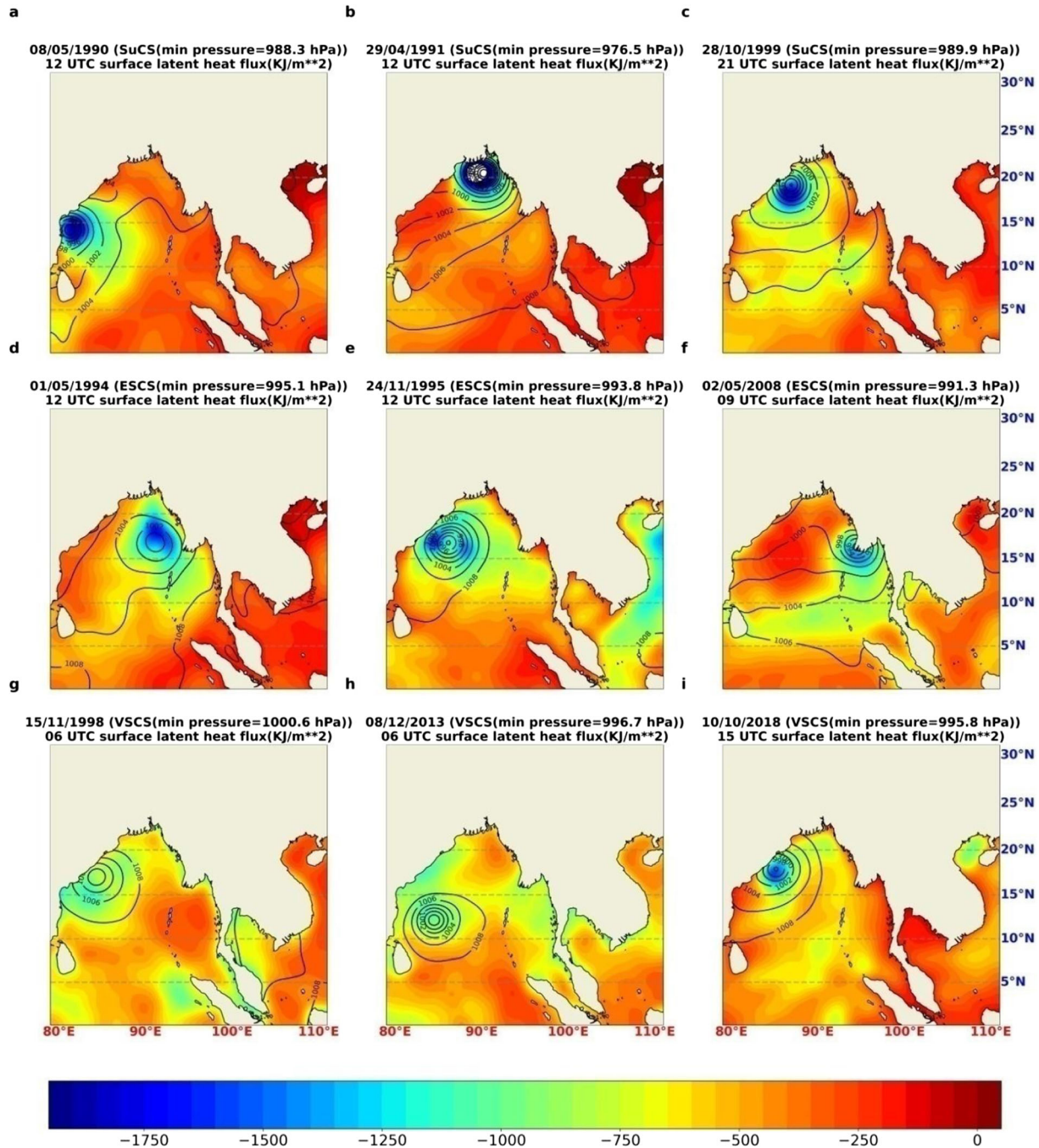


Figure 10. Pictorial example of variations of SLHF with central pressure for nine different intense TCs over BoB.

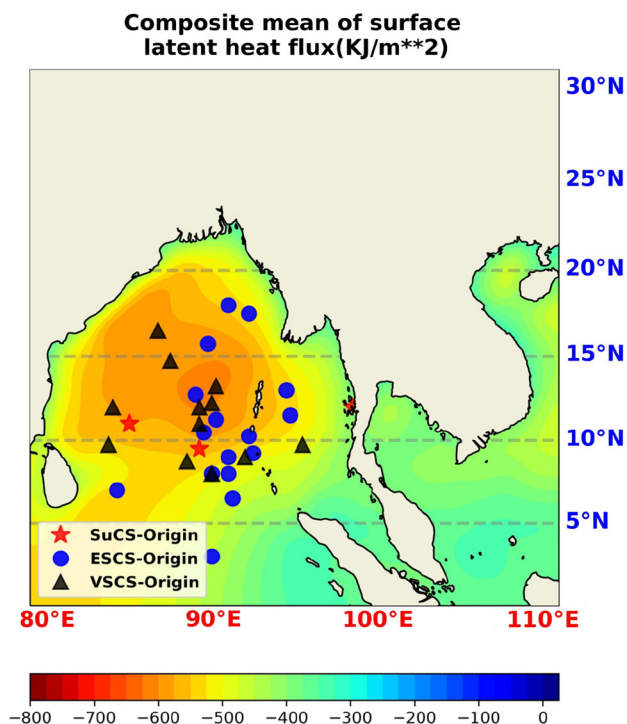


Figure 11. Composite mean of surface latent heat flux for all the intense cyclones during the period 1990–2019.

4. Conclusions

From the analysis of section 3, it is clear that the maximum number of intense TCs in the BoB form in the post-monsoon season and particularly in November. Almost 60% of these intense TCs originate in the region 8°–14°N and 88°–94°E. The composite mean of SLHF shows that the locations of higher SLHF coincide with the maximum number of genesis locations. Therefore, it can be considered an essential parameter for the genesis of TCs. The SLHF has higher values in the pre-monsoon season compared to the post-monsoon season. Almost 65% of these TCs have SLHF values between 800 and 1400 KJ m^{-2} . Out of all the parameters like SST, SLHF, MI, MRH, VWS, and 200 hPa divergence, SLHF is mostly correlated with the central pressure/max wind of intense TCs. The increase and decrease of SLHF correspond to the increase and decrease in TCs intensity. The highest SLHF corresponds to the lowest central pressure (highest wind speed) and vice versa. Thus, SLHF is the most important among the parameters discussed above for TCs intensification.

Acknowledgements

We gratefully acknowledge India Meteorological Department for encouraging us to carry out this

study. We thank anonymous reviewers for their valuable comments to improve the manuscript. We also acknowledge Somnath Naskar for helping me from time to time. The contents and views expressed in this paper are the author’s views and do not necessarily reflect the views of the organization they belong to.

Author statement

Pravat Rabi Naskar: Concept, analysis and writing. Dushmanta Ranjan Pattanaik: Writing and suggestions.

Availability of data and material

All the data used in this study have been collected from <https://www.ecmwf.int/en/forecasts/datasets/reanalysis-datasets/era5> and it is readily available there.

References

Ahmed R, Mohapatra M, Dwivedi S and Giri R K 2021 Characteristic features of Super Cyclone ‘AMPHAN’ – observed through satellite images; *Trop. Cyclone Res. Rev.* **10**(1) 16–31, <https://doi.org/10.1016/j.tcr.2021.03.003>.

Andersen T K, Radcliffe D E and Shepherd J M 2013 Quantifying surface energy fluxes in the vicinity of inland tracking tropical cyclones; *J. Appl. Meteorol. Clim.* **52** 2797–2808, <https://doi.org/10.1175/JAMC-D-13-035.1>.

Bhardwaj P and Singh O 2020 Climatological characteristics of Bay of Bengal tropical cyclones: 1972–2017; *Theor. Appl. Climatol.* **139** 615–629.

Bian G-F, Nie G-Z and Qiu X 2021 How well is outer tropical cyclone size represented in the ERA5 reanalysis dataset?; *Atmos. Res.* **249** 105339, <https://doi.org/10.1016/j.atmosres.2020.105339>.

Chavas D R, Reed K A and Knaff J A 2017 Physical understanding of the tropical cyclone wind-pressure relationship; *Nat. Commun.* **8** 1360.

Cheng C-J and Wu C-C 2020 The role of WISHE in the rapid intensification of tropical cyclones; *J. Atmos. Sci.* **77** 3139–3160, <https://doi.org/10.1175/JAS-D-20-0006.1>.

Chen S, Li W, Lu Y and Wen Z 2014 Variations of latent heat flux during tropical cyclones over the South China Sea; *Meteorol. Appl.* **21** 717–723.

Chinchole P S and Mohapatra M 2017 Some characteristics of transitional speed of cyclonic disturbances over north Indian Ocean in recent years; In: *Tropical Cyclone activity over the North Indian Ocean* (eds) Mohapatra M, Bandyopadhyay B K and Rathore L S, co-published by Capital Publishers; New Delhi and Springer, Germany, pp. 165–179.

DeMaria M 1996 The effect of vertical shear on tropical cyclone intensity change; *J. Atmos. Sci.* **53** 2076–2087.

- Emanuel K A 1986 An air–sea interaction theory for tropical cyclones. Part 1: Steady-state maintenance; *J. Atmos. Sci.* **43** 585–604, [https://doi.org/10.1175/1520-0469\(1986\)0432.0.CO;2](https://doi.org/10.1175/1520-0469(1986)0432.0.CO;2).
- Emanuel K A 1994 *Atmospheric convection*; Oxford University Press, Oxford, UK.
- Emanuel K A, Neelin J D and Bretherton C S 1994 On large-scale circulations in convective atmospheres; *Q.J.R.M.S.* **120** 519, <https://doi.org/10.1002/qj.49712051902>.
- Emanuel K, DesAutels C, Holloway C and Korty R 2004 Environmental control of tropical cyclone intensity; *J. Atmos. Sci.* **61**(7) 843–858, [https://doi.org/10.1175/1520-0469\(2004\)0612.0.CO;2](https://doi.org/10.1175/1520-0469(2004)0612.0.CO;2).
- Flotz G R, Balaguru K and Hagos S 2018 Interbasin differences in the relationship between SST and tropical cyclone intensification; *Mon. Weather Rev.* **146** 853–870, <https://doi.org/10.1175/MWR-D-17-0155.1>.
- Ganesh S S, Sahai A K, Abhilash S, Joseph S, Kaur M and Phani R 2020 An improved cyclogenesis potential and storm evolution parameter for North Indian Ocean; *Earth Space Sci.* **7**(10), <https://doi.org/10.1029/2020EA001209>.
- Gao S and Chiu L S 2010 Surface latent heat flux and rainfall associated with rapidly intensifying tropical cyclones over the western North Pacific; *Int. J. Remote Sens.* **31**(17–18) 4699–4710, <https://doi.org/10.1080/01431161.2010.485149>.
- Gelaro *et al.* 2017 The Modern-Era Retrospective Analysis for Research and Applications, Version 2 (MERRA-2); *J. Clim.* **30** 5419–5454, <https://doi.org/10.1175/JCLI-D-16-0758.1>.
- Gray W M 1968 Global view of the origin of tropical disturbances and storms; *Mon. Weather Rev.* **96** 669–700.
- Gray W M 1979 Hurricanes: Their formation, structure, formation and likely role in the tropical circulation; In: *Meteorology over the tropical oceans* (ed.) Shaw D B, Reading, UK; *R. Meteorol. Soc.* 155–218.
- Gray W M 1998 The formation of tropical cyclones; *Meteorol. Atmos. Phys.* **67** 37–69, <https://doi.org/10.1007/BF01277501>.
- Harikumar R *et al.* 2022 Ocean state forecasting during VSCS Ockhi and a note on what we learned from its characteristics: A forecasting perspective; *J. Earth Syst. Sci.* **131** 92, <https://doi.org/10.1007/s12040-022-01850-z>.
- Hersbach H and Dee D 2016 ERA5 reanalysis is in production; *ECMWF Newsllett.* **147**(7).
- Kotal S D, Kundu P K and Roy Bhowmik S K 2009 An analysis of cyclogenesis parameter for developing and non-developing low pressure systems over the Indian Sea; *Nat. Hazards* **50** 389–402.
- Kumar S V J, Ashthikar S S and Mohapatra M 2017 Life period of cyclonic disturbances over the North Indian ocean during recent years; In: *Tropical cyclone activity over North Indian Ocean* (ed.) Mohapatra M, Bandyopadhyay B K and Rathore L S, co-published by Capital Publishers, New Delhi and Springer, Germany, pp. 181–198.
- Lavender S L, Hoeke R K and Abbs D J 2018 The influence of sea surface temperature on the intensity and associated storm surge of tropical cyclone Yasi: A sensitive study; *Nat. Hazards Earth Syst. Sci.* **18** 795–805.
- Lengaigne M, Neetu S, Samson G, Vialard J, Krishnamohan K S, Masson S, Jullien S, Suresh I and Menkes C E 2019 Influence of air–sea coupling on Indian Ocean tropical cyclones; *Clim. Dyn.* **52** 577–598, <https://doi.org/10.1007/s00382-018-4152-0>.
- Li G, Ren B, Yang C and Zheng J 2011 Revisiting the trend of the tropical and subtropical Pacific surface latent heat flux during 1977–2006; *J. Geophys. Res.* **116** D10115.
- Malakar P, Kesarkar A P, Bhate J N, Singh V and Deshamukhya A 2020 Comparison of Reanalysis Data Sets to comprehend the evolution of Tropical Cyclones over North Indian Ocean; *Earth Space Sci.* **7** e2019EA000978, <https://doi.org/10.1029/2019EA000978>.
- Manganello J V *et al.* 2012 Tropical cyclone climatology in a 10-km global atmospheric GCM: Toward weather-resolving climate modeling; *J. Clim.* **25**(11) 3867–3893, <https://doi.org/10.1175/JCLI-D-11-00346.1>.
- Mohanty S, Nadimpalli R, Osuri K K, Pattanayak S, Mohanty U C and Sil S 2019 Role of sea surface temperature in modulating life cycle of tropical cyclones over Bay of Bengal; *Trop. Cyclone Res. Rev.* **8**(2) 68–83, <https://doi.org/10.6057/2019TCRR02.02>.
- Mohapatra M and Sharma M 2021 Comparative analysis of vital parameters of extremely severe cyclonic storms Phailin and Hudhud over the Bay of Bengal; *J. Earth Syst. Sci.* **130** 233, <https://doi.org/10.1007/s12040-021-01719-7>.
- Mohapatra M, Bandyopadhyay B K, Ray Kamaljit and Rathore L S 2014 Early warning services for management of cyclones over North Indian Ocean: Current status and future scope; In: *High impact weather events over SAARC Region* (ed.) Ray K, Mohapatra M, Bandyopadhyay B K and Rathore L S, Capital Publishing Co. and Springer Publications Ltd.
- Montgomery M T and Farrell B F 1993 Tropical Cyclone formation; *J. Atmos. Sci.* **50** 285–310.
- Montgomery M T, Snag N V, Smith R K and Persing J 2009 Do tropical cyclones intensify by WISHE?; *Quart. J. Roy. Meteorol. Soc.* **135** 1697–1714, <https://doi.org/10.1002/qj.459>.
- Naskar P R and Naskar S 2021 Synoptic and dynamical characteristics of super cyclone Amphan; *Mausam* **72**(1) 237–252.
- Neumann C J 1993 Global overview; In: *Global guide to tropical cyclone forecasting*, World Meteorological Organization, Geneva, pp. 1.1–1.56.
- Ooyama K 1969 Numerical simulation of the life cycle of tropical cyclones; *J. Atmos. Sci.* **26** 1586–1606.
- Palmen E 1948 On the formation and structure of tropical hurricanes; *Geophysica* **3** 26–38.
- Park M-S, Elsberry R L and Harr P A 2012 Vertical wind shear and ocean heat content as environmental modulators of Western North Pacific Tropical Cyclone intensification and decay; *Trop. Cyclone Res. Rev.* **1**(4) 448–457.
- Pielke R A and Pielke R A S 1997 *Hurricanes: Their nature and impacts on society*; John Wiley and Sons, 279p.
- Rappin E D, Morgan M C and Tripoli G J 2011 The impact of outflow environment on tropical cyclone intensification and structure; *J. Atmos. Sci.* **68** 177–194.
- Ren D, Lynch M, Leslie L M and Lemarshall J 2014 Sensitivity of tropical cyclone track and intensity to ocean surface temperature: Four cases in four different basins; *Tellus A* **64** 24212.
- Reshmi Mohan P, Srinivas C V, Yesubabu V, Rao V B, Vittal Murthy K P R and Venkatraman B 2022 Impact of SST on the intensity prediction of extremely severe tropical cyclones Fani and Amphan in the Bay of Bengal; *Atmos.*

- Res. **273** 106151, <https://doi.org/10.1016/j.atmosres.2022.106151>.
- Riehl H 1950 A model of hurricane formation; *J. Appl. Phys.* **21** 917–925, <https://doi.org/10.1063/1.1699784>.
- Sanap S D, Mohapatra M, Ali M M, Priya P and Varaprasad D 2020 On the dynamics of cyclogenesis, rapid intensification and recurvature of the very severe cyclonic storm, Ockhi; *J. Earth Syst. Sci.* **129** 194, <https://doi.org/10.1007/s12040-020-01457-2>.
- Simpson R, Anthes R A and Garstang M 2002 Hurricane! Coping with disaster: Progress and challenges since Galveston; *Amer. Geophys. Union.*, 360p.
- Singh O P 2007 Long-term trends in the frequency of severe cyclones of Bay of Bengal: Observations and simulations; *Mausam* **58**(1) 59–66.
- Singh V K and Roxy M K 2022 A review of ocean-atmosphere interactions during tropical cyclones in the north Indian Ocean; *Earth-Sci. Rev.* **226** 103967, <https://doi.org/10.1016/j.earscirev.2022.103967>.
- Singh V K, Roxy M K and Deshpande M 2020 The unusual long track and rapid intensification of very severe cyclone Ockhi; *Curr. Sci.* **119**(5) 771–779, <https://doi.org/10.18520/cs/v119/i5/771-779>.
- Srinivas C V, Mohan G M, Naidu C V, Baskaran R and Venkatraman B 2016 Impact of air–sea coupling on the simulation of tropical cyclones in the North Indian Ocean using a simple 3-D Ocean model coupled to ARW; *J. Geophys. Res. Atmos.* **121** 9400–9421, <https://doi.org/10.1002/2015JD024431>.
- Sun Y, Zhong Z, Li T, Yi L, Hu Y, Wan H, Chen H, Liao Q, Ma C and Li Q 2017 Impact of ocean warming on tropical cyclone size and its destructiveness; *Sci. Rep.* **7** 8154.
- Vincent E M, Lengaigne M, Madec G, Vialard J, Samson G, Jourdain N, Menkes C E and Jullien S 2012a Processes setting the characteristics of sea surface cooling induced by tropical cyclones; *J. Geophys. Res.* **117** C02020, <https://doi.org/10.1029/2011JC007396>.
- Vincent E M, Lengaigne M, Vialard J, Madec G, Jourdain N and Masson S 2012b Assessing the oceanic control on the amplitude of sea surface cooling induced by tropical cyclones; *J. Geophys. Res.* **117** C05023, <https://doi.org/10.1029/2011JC007705>.
- Vinod K K, Soumya M, Tkalich P and Vethamony P 2014 Ocean–atmosphere interaction during thane cyclone: A numerical study using WRF; *Indian J. Geomar. Sci.* **43** 1230–1235.
- Vishwakarma V, Pattanaik S, Chakraborty T, Joseph S and Mitra A K 2022 Impacts of sea-surface temperatures on rapid intensification and mature phases of super cyclone Amphan (2020); *J. Earth Syst. Sci.* **131** 60, <https://doi.org/10.1007/s12040-022-01816-1>.
- Yu L and Weller R A 2007 Objectively analyzed air–sea heat fluxes for the global ice-free oceans (1981–2005); *Bull. Am. Meteorol. Soc.* **88** 527–539.
- Zhang F and Emanuel K 2016 On the role of surface fluxes and WISHE in Tropical Cyclone intensification; *J. Atmos. Sci.* **73** 2011–2019, <https://doi.org/10.1175/JAS-D-16-0011.1>.
- Zhou L-T, Chen G and Wu R 2015 Change in surface latent heat flux and its association with tropical cyclone genesis in the western North Pacific; *Theor. Appl. Climatol.* **119** 221–227, <https://doi.org/10.1007/s00704-014-1096-0>.
- Springer Nature or its licensor (e.g. a society or other partner) holds exclusive rights to this article under a publishing agreement with the author(s) or other rightsholder(s); author self-archiving of the accepted manuscript version of this article is solely governed by the terms of such publishing agreement and applicable law.

Corresponding editor: T NARAYANA RAO